Dilatometry of Dipalmitoyllecithin–Cholesterol Bilayers†

Donald L. Melchior,*‡ Francis J. Scavitto, and Joseph M. Steim*

ABSTRACT: The interactions of cholesterol and dipalmitoylphosphatidylcholine in bilayers were investigated by differential scanning dilatometry and related techniques. Dipalmitoylphosphatidylcholine bilayers ranging from 0 to 50 mol % cholesterol were studied over a temperature range of 0–50 °C. These investigations allowed construction of a three-dimensional surface with dimensions of mole fraction of cholesterol, temperature, and apparent partial specific volume. Much of the phenomenology reported for dipalmitoylphosphatidylcholine and dipalmitoylphosphatidylcholine–cholesterol bilayers appears and can be interrelated on this surface. In addition to the thermotropic events associated with the system, two cholesterol-induced events at 17.5–20 and 29 mol % cholesterol are particularly in evidence.

The nature of cholesterol–phospholipid interaction in bilayers is little understood. Early studies revealed that cholesterol condenses fluid phospholipid monolayers while fluidizing solid ones (Shah & Schulman, 1967). Subsequent DSC[1] demonstrated that cholesterol suppresses the bilayer order/disorder transition (Ladbrooke et al., 1968), in which the bilayers go from a fluid state at higher temperatures to a crystalline-like state at lower temperatures (Ranck et al., 1974). Sufficient cholesterol in a bilayer serves as a plasticizer, causing the bilayer to exist in a state intermediate between crystalline and fully fluid [for a review, see Demel & de Kruyff (1976)], and the suppression of the bilayer transition is a reflection of this state of intermediate fluidity. In cholesterol-rich bilayers, simple processes such as transbilayer diffusion of water (Bittman & Blau, 1972) or more complex processes such as protein-mediated sugar transport (Melchior & Czech, 1979) are enhanced relative to crystalline bilayers but reduced relative to fully fluid bilayers. Studies on membranes of living cells are in agreement with studies on model membranes (Razin & Rottem, 1978; Melchior & Steim, 1979).

The molecular interaction of cholesterol with phospholipids has been studied intensely (Demel & de Kruyff, 1976; Huang, 1977; Green, 1977). One approach has been to use physical techniques, including DSC (Ladbrooke et al., 1968; Hinz & Sturtevant, 1972; Estep et al., 1978; Mabrey et al., 1978), X-ray diffraction (Engelman & Rothman, 1972), NMR (Phillips & Finer, 1974; Opella et al., 1976; Brûlet & McConnell, 1976; Habercorn et al., 1977), ESR (Shimshick & McConnell, 1973; Rubinstein et al., 1980), EM (Verkleij et al., 1974; Hui & Parsons, 1975; Gebhardt et al., 1977; Copland & McConnell, 1980), and equilibrium sedimentation (Gershfeld, 1978), to monitor the properties of bilayers as a function of cholesterol content. The results of many of these studies have appeared contradictory. Apparent associations of cholesterol with phospholipids in stoichiometric ratios of 1:4, 1:2, or 1:1 are suggested. Recently, it has been shown that the lateral diffusion coefficient of fluorescent-labeled phospholipids in PC bilayers increases greatly at around 20 mol % cholesterol (Rubenstein et al., 1979).

Dilatometry, although not yet widely employed, has nonetheless also proven useful in lipid bilayer studies (Sheetz & Chan, 1972; Nagle & Wilkinson, 1978; MacDonald, 1978). Like DSC (Steim, 1974; Scheidler & Steim, 1975), scanning dilatometry provides thermodynamic information and requires no probe molecules with their disadvantages (Melchior & Steim, 1976). Furthermore, apparent partial specific volumes may be more directly interpretable in terms of molecular associations than the apparent heat capacities given by DSC (Melchior et al., 1977). Because of the potential usefulness of dilatometry in biomembrane studies, we have developed a differential scanning dilatometer, which, together with auxillary techniques, allows us to continuously measure partial specific volumes as a function of time or temperature (Blazyk et al., 1975; Melchior et al., 1977).

Using this instrument, we have constructed a three-dimensional X_c–T–$\bar{V}_a$ surface for the DPPC–cholesterol bilayer in excess water. The portion of the surface presented here, extending from 0 to 50 mol % cholesterol and from 0 to 50 °C, demonstrates much of the phenomonology associated with increasing cholesterol content in bilayers and ties together much disparate phenomena observed by other techniques. A most striking event, strongly suggesting a phase boundary, occurs between 17.5 and 20 mol % cholesterol below the bilayer order/disorder transition. It is most likely responsible for the large alterations in the lateral diffusion coefficients of fluorescent probes observed in lecithin bilayers over this range of cholesterol content (Rubenstein et al., 1979).

Materials and Methods

Materials. DPPC, DOPC, and cholesterol were purchased from Sigma (St. Louis, MO). Each lot of DPPC and DOPC was examined for purity by TLC on silica gel G plates using chloroform–methanol–water (65:25:4), with detection by Dittmer reagent (Vaskovsky & Kastetsky, 1968) and sulfuric acid–dichromate charring. Lots selected for use gave a single spot with conventional sample size, but on grossly overloaded plates a trace of phosphorus-positive material was seen just leading the PC region; it contained less than 1% of the PC phosphorus. DSC of DPPC showed a sharp transition and premelt at the appropriate temperatures. Cholesterol was recrystallized 3 times from ethanol shortly before use and dried in vacuo at room temperature. It was chromatographically

† From the Department of Chemistry, Brown University, Providence, Rhode Island 02912. *Received May 19, 1980.* This work was supported by the National Institutes of Health under Grant GM 20545.

‡ Recipient of an American Diabetes Association, Inc., Research and Development Award.

[1] Abbreviations used: DSC, differential scanning calorimetry; $\bar{V}_a$, apparent partial specific volume; α, volume coefficient of expansion; X_c, mole fraction of cholesterol (in mole percent); PC, phosphatidylcholine; DPPC, L-α-dipalmitoylphosphatidylcholine; DMPC, L-α-dimyristoylphosphatidylcholine; DOPC, L-α-dioleoylphosphatidylcholine.

0006-2960/80/0419-4828$01.00/0

homogeneous by TLC on silicic acid when developed and detected by charring.

Sample Preparation. For each run PC was dried overnight under vacuum (100 μmHg) at 90 °C and weighed. The desired amount of cholesterol in redistilled reagent grade chloroform was then added, and the solution was transferred with several washings of chloroform into a 100-mL round-bottom flask. The chloroform was evaporated off under a stream of N_2 while the flask was swirled in a 55 °C water bath, and when the lipid was dried to a thin film, the remaining chloroform was removed under vacuum (100 μmHg) at room temperature overnight. The lipid was dispersed in approximately 8 mL of deionized distilled water by swirling with glass beads in a 55 °C water bath until a homogeneous dispersion was obtained. After dispersion the flask was cooled under a stream of cool water to room temperature before degassing prior to dilatometry or diluting for density gradient centrifugation.

Differential Scanning Dilatometry. Samples, ranging from about 90 to 200 mg dry weight, were degassed, loaded, and run in the dilatometer as previously described (Melchior et al., 1977) at a scan rate of 8 °C/h. The samples were scanned up from 0 to 53 °C, held for 1 h at 53 °C, then scanned down to 0 °C. Samples were carried through this cycle a second and even third time. Repeated runs were superimposable. Even in the extreme case of samples repeatedly run over a period of 4 days, all runs were identical. TLC performed on samples after 4 days in the dilatometer showed slight traces of lyso-PC formation.

Dry Weight Determination. After dilatometry, samples were removed from the dilatometer cell by rinsing several times with distilled water into a glass-stoppered flask and weighed. After thorough mixing, aliquots of about 1 mL of the diluted samples (~5 mg of lipid) were weighed into tared sample pans. Dry weights were taken to an error of ±1 μg, using a recording dry weight apparatus together with procedures described elsewhere (Melchior et al., 1977), at 1000 μmHg and 70 °C until constant mass was obtained. Higher temperatures and lower pressures were found to cause sublimation of cholesterol. All dry weights were performed in triplicate.

Data Treatment. Raw data were processed as previously described (Melchior et al., 1977). For removal of the small amount of noise present in any run, $\bar{V}_a$ vs. T curves were smoothed with least-squares fits on an IBM 370/148 computer using the method of cubic splines with optimized knot locations (Ahlberg et al., 1967). Values of $\bar{V}_a$ derived from the continuous dilatometer output were taken at 0.5 °C intervals and were recalculated over these same intervals by using the equations obtained by the method of cubic splines. All dilatometric data presented are taken from the smoothed curves.

Values of the coefficient of expansion, α, given by $(1/\bar{V})(d\bar{V}/dT)$, were calculated from $\bar{V}_a$ vs. T curves. At any temperature, T, α was calculated by subtracting the value of $\bar{V}_a$ 0.5 °C below T from its value 0.5 °C above T and dividing by the value of $\bar{V}_a$ at T. Since α is calculated over 1 °C intervals, peaks in plots of α vs. T are computationally broadened. Occasional sudden slope changes in α vs. T plots are also the consequence of plotting at discrete 0.5 °C intervals. Values for $\Delta\bar{V}_a$ were calculated in the manner described by Nagle & Wilkinson (1978).

Density Gradients. Gradients were formed with a gradient generator, starting with 5.0 mL of D_2O in the mixing chamber and 5.5 mL of H_2O in the reservoir. A peristalic pump at a flow rate of 1.2 mL/min delivered 5.5 mL of the desired portion of the gradient into 0.5 × 2 in. centrifuge tubes. The gradients were confirmed to be consistently linear and reproducible by measuring the gradient of optical density at 589 nm formed by replacing the water in the reservoir by a solution of crystal violet at pH 7.0. Crystal violet obeyed Beer's law over the concentration range used. Isopycnic gradient centrifugation was carried out at 9 °C and 30 K rpm for 3 h in a Beckman SW 39 rotor, and the density of the lipid band was confirmed by measuring the refractive index of the gradient immediately above, within, and below the band. The resulting bands were sharp, never exceeding 1 mm. Fractions of 0.5 mL were collected and measured at 4 °C for band density determination.

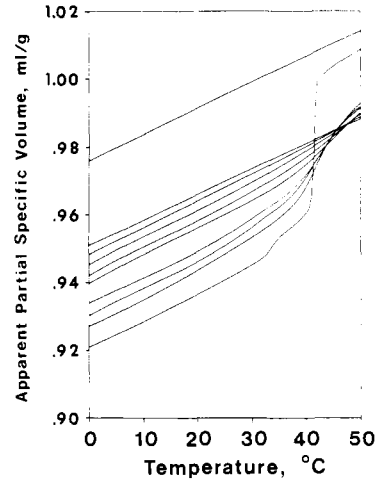

FIGURE 1: Temperature dependence of the apparent partial specific volume ($\bar{V}_a$) for pure DPPC and DOPC bilayers and a series of cholesterol-containing DPPC bilayers. The featureless curve with the highest $\bar{V}_a$ is that of DOPC. Pure DPPC is the curve with the lowest $\bar{V}_a$ at low temperatures. The remaining curves, from the bottom up at lower temperatures, are for DPPC bilayers containing 20, 23, 25, 29, 33, 40, 45, and 50 mol % cholesterol.

Flotation–Sedimentation Experiments. Acid-cleaned, screw-top culture tubes were sylonated by coating with Syl-on-HTP (Supelco, PA) for 15 min and were then thoroughly rinsed with chloroform, with methanol, and with water. The tubes were then dried. To each tube was added an aliquot of an H_2O–D_2O mixture of an appropriate density chosen from Figure 3. The tubes were capped with Teflon-lined caps and heated to 60 °C, and the lipids were suspended by agitation on a vortex mixer. The suspensions were finally degassed in vacuo, sealed in a helium atmosphere, left at 4 °C overnight, and then thermostated in the water bath. In most tubes the rates of sedimentation or flotation were greatly enhanced because of flocculation of the lipid particles, but in any case a pattern could be seen within 1 day. Because of the different coefficients of expansion of the lipids and the H_2O–D_2O mixtures, adjusting the bath temperature by a few degrees allowed the densities of the entire concentration range to be explored.

Results

Figure 1 shows the temperature dependency of $\bar{V}_a$ for a series of cholesterol-containing DPPC bilayers and for pure DPPC and DOPC bilayers. DOPC has its order/disorder transition at −28 °C (Melchior & Steim, 1976) and is therefore fully fluid over the temperature range of 0–50 °C. It is seen in Figure 1 as the featureless curve with the highest partial specific volume. No indication of any event occurring below ca. 30 °C, as reported by spin-label studies (Lee et al., 1974), is seen dilatometrically. The remaining curves in Figure 1 are those of DPPC and cholesterol-containing DPPC bilayers. Pure DPPC gives the lowest $\bar{V}_a$ at low temperatures. Its

features agree well with previous dilatometric studies of pure DPPC (Sheetz & Chan, 1972; Blazyk et al., 1975; Melchior et al., 1977; Nagle & Wilkinson, 1978; McDonald, 1978). The discontinuities in slope at the sharp main transition are artifacts arising because the continuous raw data were digitalized at discrete 0.5 °C intervals. The raw analogue record reveals the main transition to be centered at 41.6 °C, with a half-width of about 0.1 °C. The $\Delta\bar{V}_a$ for the main transition is 0.0383 mL g^{-1}, which corresponds to an increase in bilayer volume of 4.0%. The pretransition (Hauser & Phillips, 1979) occurs over a temperature range of about 33–35 °C, with a $\Delta\bar{V}_a$ of 0.002 mL g^{-1} (0.21%). As described in a previous publication (Melchior et al., 1977), the premelt is subject to hysteresis and occurs at lower temperatures in downscans than in upscans. All data treated in this publication are obtained from upscans carried out at a heating rate of 8 °C/h.

The remaining curves in Figure 1, reading from the bottom up at lower temperatures, are for 20, 23, 25, 29, 33, 40, 45, and 50 mol % cholesterol. Samples containing 2, 5, 7, 10, 15, and 17 mol % were also run and are presented as part of Figure 3. In Figure 1 the general trend of the suppression of the main transition with increasing X_c is readily apparent. As will become particularly apparent in coefficients of expansion to be presented later, a narrow component closely resembling that found in pure DPPC is present when $X_c \lesssim 17$; it decreases in intensity with added cholesterol in the range $0 < X_c \lesssim 17$ but can be discerned easily at $X_c = 15$. By $X_c = 20$, no trace of the narrow component can be found, but a broad transition remains until at least $X_c = 40$. At $X_c = 50$, where no transitions appear to be present, $\bar{V}_a$ is approximately midway between that of unmelted and fully fluid bilayers of pure DPPC. Note that below about 30% cholesterol the curves are nearly parallel straight lines. However, unexpected downward curvature at temperatures less than about 5 °C can be seen in some plots (X_c = 23, 29, 33, and 40) by sighting down the lines. Since this effect occurs during the first 0.5 h of an upscan but disappears on a downscan, it may be an artifact reflecting the time required by the dilatometer to achieve steady-state conditions.

The detailed structure of $\bar{V}_a$ is best seen by examining the coefficient of expansion α, given by $(1/\bar{V})(d\bar{V}/dT)$, as a function of temperature. This mode of presentation also facilitates comparing the dilatometric data with previously published calorimetric studies. The curves displayed in Figure 2 were obtained from $\bar{V}_a$ as described under Materials and Methods. As in Figure 1, discontinuities in the slopes arise because the recorder output was digitalized at discrete 0.5 °C intervals; this procedure may also slightly broaden the sharper peaks in the curves for $0 \leq X_c \leq 15$.

Figure 2a shows α for pure DPPC bilayers; the pretransition and main transition resemble those observed by differential scanning calorimetry. DPPC bilayers containing 2 mol % cholesterol (Figure 2b) have a broadened pretransition, but, within the limitations of the data, the width of the main transition is unchanged. Calculated directly from the recorder output, for $X_c = 2$ the temperature of the narrow main transition is shifted down almost a degree from its value in pure DPPC. Additional cholesterol seems to cause only a slight additional down shift. When $X_c = 5$ (Figure 2c), the pretransition is broadened further and runs into the main transition. Dilatometric scans, not shown in Figure 2, were also performed for 7 and 10% cholesterol. Indications of the pretransition are still evident at 7% but were absent at 10%. Runs made on our modified Perkin-Elmer DSC 2 calorimeter showed that the premelt became undetectable in DPPC bi-

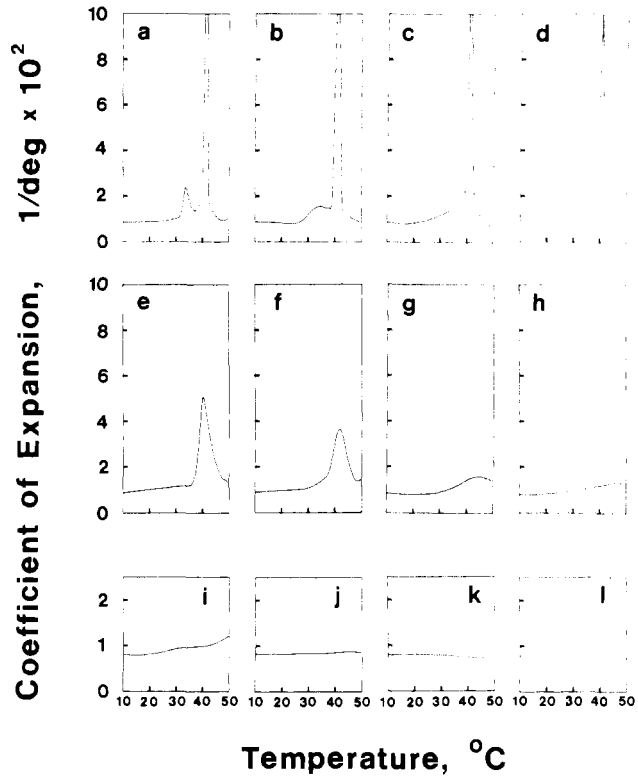

FIGURE 2: Temperature dependence of the coefficient of expansion (α) for DPPC bilayers containing (a) 0, (b) 2, (c) 5, (d) 15, (e) 17, (f) 20, (g) 29, and (h) 33 mol % cholesterol. Shown on an expanded scale is α for DPPC bilayers containing (i) 40, (j) 45, and (k) 50 mol % cholesterol and for (l) pure DOPC bilayers.

layers containing between 7 and 9% cholesterol. It is difficult, however, to determine at what X_c the pretransition vanishes, since the broadened pretransition gradually blends into the onset of the main transition.

Comparison of Figures 2c and 2b suggests that the high-temperature tail of the sharp peak may be changing even at $X_c = 5$. Curves of X_c of 7 and 10 (not shown) exhibit a progressively increasing change in this region. By $X_c = 15$ (Figure 2d) not only has the pretransition vanished but in place of the main transition a remaining narrow component appears to be superimposed upon a second, broader peak which is particularly evident in the high-temperature tail. The narrow component, still resembling that of pure DPPC, is less in height and area than in the preceding figures.

At $X_c = 17$ (Figure 2e) no narrow component is observed, although the asymmetry of the peak suggests that it still may make a small contribution. Nevertheless, the nature of the broad peak underlying the narrow component at lower concentrations of cholesterol is revealed. It is about 12 °C wide, beginning at about 35 °C and ending at about 47 °C. Its maximum at 40.0 °C, unshifted from Figure 2d, and may in part be determined by a contribution from traces of a remaining narrow component. At $X_c = 20$ (Figure 2f) the broad peak is symmetrical, with a maximum at about 41.5 °C, 1.5 °C higher than that for $X_c = 17$; its onset appears to occur at a lower temperature. Further additions of cholesterol underscore the tendency of this transition to broaden, shift up in temperature, and decrease in size with increasing X_c. At $X_c = 29$ (Figure 2g) the maximum occurs at about 45 °C, while the onset, although vaguely defined, is at about 26 °C. At $X_c = 33$, the maximum has moved to about 47 °C while the onset may be as low as 15 °C. A plot of maximum temperatures against X_c is linear, with a slope of 0.44 °C $\%^{-1}$.

Coefficients of expansion for higher percentages of chole-

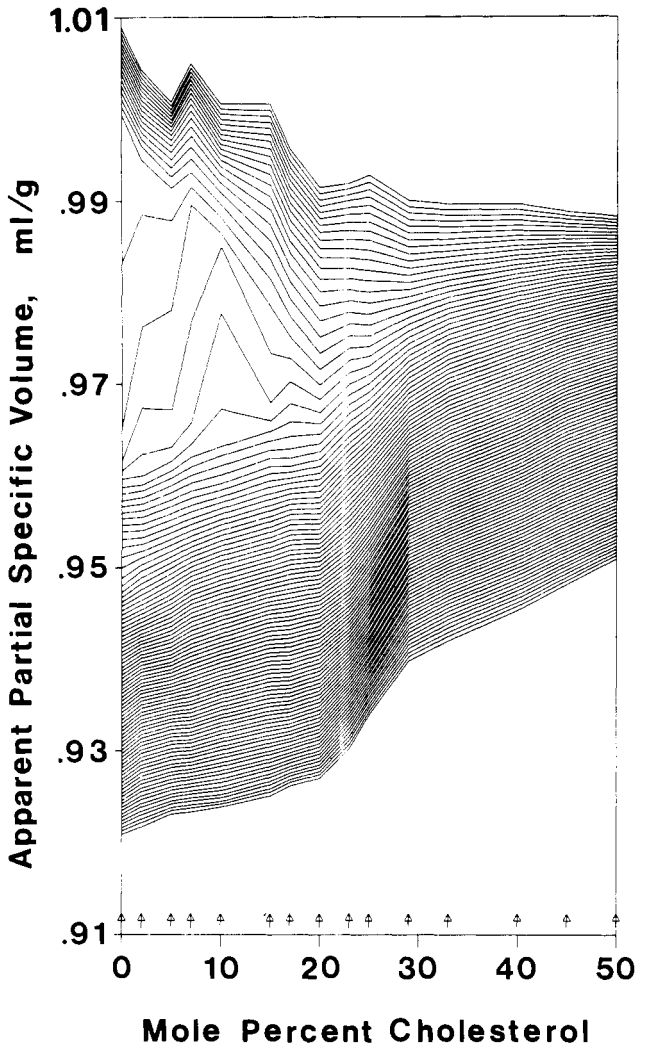

FIGURE 3: Apparent partial specific volume ($\bar{V}_a$) of pure and cholesterol-containing DPPC bilayers over the temperature range of 0–50 °C. $\bar{V}_a$ is plotted against mole percent cholesterol (X_c) at 0.5 °C temperature intervals extending from 0 (bottom) to 50 °C (top). The concentration of bilayer cholesterol in the dilatometer runs used to construct the plots is indicated by the 15 arrows along the X_c axis at X_c = 0, 2, 5, 7, 10, 15, 17, 20, 23, 25, 29, 33, 40, 45, and 50. Experimental points at these concentrations are connected by straight lines. Since vertical cuts at the arrows reproduce the experimental volume–temperature curves, the vertical spacings between the lines are a measure of the coefficient of expansion at various cholesterol concentrations.

sterol are shown on an expanded scale in the last row of Figure 2. At X_c = 40 (Figure 2i) a very broad but weak transition remains, with a maximum beyond 50 °C; we believe the depression in α in the neighborhood of 40 °C may be an artifact since its magnitude is close to the sensitivity of our dilatometer. The transition can also be seen easily in Figure 1 with the aid of a straightedge or by sighting along the 40% line. Beyond X_c = 40, the persistence of a very broad transition cannot be determined with certainty. At X_c = 45 (Figure 2j) there is the suggestion of a transition, but the effect is near the limits of precision of the measurements. On the other hand, note that the slope of α for pure DOPC (Figure 2l) is slightly negative; this lipid is thought to have no transition over the temperature range studied. If the negative slope for DOPC is real, then the negative slope for X_c = 50 (Figure 2k) may also be real, and comparison of Figures 2j and 2k may indicate presistence of a broad transition up to at least X_c = 45. A very broad transition extending to about 50% cholesterol has

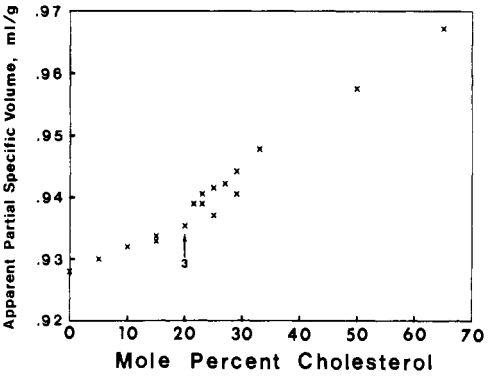

FIGURE 4: Apparent partial specific volume of pure and cholesterol-containing DPPC bilayers at 9 °C as determined by D_2O–H_2O isopycnic gradient centrifugation. All bands were sharp, never exceeding 1 mm. The point at 20 mol % cholesterol represents three separate runs.

been found by calorimetry (Mabrey et al., 1978).

The dilatometer results are presented in an alternative way in Figure 3, where $\bar{V}_a$ is plotted against X_c at 0.5 °C temperature intervals from 0 (bottom) to 50 °C (top). The concentrations of bilayer cholesterol in the dilatometer runs used to construct the plots are indicated by the 15 arrows along the X_c axis at 0, 2, 5, 7, 10, 15, 17, 20, 23, 25, 29, 33, 40, 45, and 50 mol % and include the scans of Figure 1. Experimental points at these concentrations are connected by straight lines. Since vertical cuts at the arrows reproduce the experimental volume–temperature curves, the vertical spacings between the lines are a measure of the coefficients of expansion at various cholesterol concentrations. Thus, the phenomena already discussed can be seen by scanning Figure 3 in the ordinate direction. At $0 \leq X_c \leq 20$ an abrupt change in $\bar{V}_a$ occurs in the neighborhood of 40 °C but decreases in size until $X_c \simeq 20$; above this cholesterol concentration a broad transition remains until nearly 50 mol %.

However, plotting against X_c reveals additional information obscured by the preceding presentations. The dominant features are best described by considering the temperature regions below the DPPC transition near 40 °C, above the transition, and the transition itself. Below the transition, where pure DPPC is ordered, $\bar{V}_a$ increases with increasing X_c. This effect is not surprising in view of the well-known fluidizing effect of cholesterol upon lecithin bilayers below T_c. However, closer inspection of any isotherm reveals at least three distinct segments. In this lower temperature region over the cholesterol concentration range of $0 \leq X_c \leq 20$, the bilayers expand linearly as X_c increases, with a slope of 2.6×10^{-4} mL g^{-1} $\%^{-1}$. At $29 \leq X_c \leq 50$, expansion continues with increasing X_c, but at a greater rate of 4.9×10^{-4} mL g^{-1} $\%^{-1}$. Thus, it appears that the mode of association of the sterol with the lecithin below $X_c \simeq 20$ differs from that above X_c = 29. A third distinct segment of even greater slope (17×10^{-4} mL g^{-1} $\%^{-1}$) occurs at $20 \leq X_c \leq 29$. Thus, two events appear to take place: one at about 20% cholesterol and another at about 29%.

The general form of the isotherms in this lower temperature region was verified by isopycnic centrifugation in linear H_2O–D_2O gradients at 9 °C as described under Materials and Methods. The results, shown in Figure 4, are consistent with Figure 3. $\bar{V}_a$ increases with increasing cholesterol content, and the rate of expansion below $X_c \simeq 20$ is less than that above $X_c \simeq 29$. The slopes of these two segments (3.5×10^{-4} and 6.3 mL g^{-1} $\%^{-1}$) are greater than those seen by dilatometry, but precise numerical agreement is not expected because of inherent inaccuracies, such as the lack of good temperature control in the centrifuge. For all points plotted in Figure 4,

the bands produced in the density gradient runs were compact (~1 mm wide), well-defined, and thus apparently consisted of particles of uniform density. The point at $X_c = 65$ is included because it met this criterion; the band produced by $X_c = 75$ was broad and ill-defined. Apparently density hemogeneity depends upon the method of preparation. Dispersions prepared by the method of dialysis from methanol into water produced broad, ill-defined bands even at low concentrations of cholesterol.

In the temperature region of Figure 3 above the major thermal transition, where bilayers of DPPC are fluid, the condensing effect of cholesterol produces a pronounced negative slope at the lower concentrations of cholesterol. Unfortunately, severe scatter of unknown origin precludes precise analysis of Figure 3 at high temperatures and low cholesterol concentrations. Nevertheless, it is clear that a change in slope occurs at about 20 mol % cholesterol both above and below the DPPC order/disorder transition. If it is assumed that the data in the range $0 \leq X_c \leq 20$ can be fit with a straight line, a slope of -7.5×10^{-4} mL g^{-1} % is obtained. It might be argued from the data that a third region exists at $20 \leq X_c \leq 29$, just as it does at lower temperatures, but the imprecision is too great to allow a definite conclusion to be drawn. Above $X_c \simeq 29$ the slope, although still negative, is lessened. At about 48 °C and $X_c \simeq 29$, $\bar{V}_a$ is independent of cholesterol concentration.

The most dominant feature of Figure 3 is the order/disorder transition of DPPC in the neighborhood of 40 °C. The volume change accompanying the transition is greatest for pure DPPC at $X_c = 0$ and decreases with increasing cholesterol concentration. Note that the four isotherms which trace the most abrupt portions of the volume change (the narrow peaks of parts a–d of Figure 2) rise to a maximum at about $X_c = 10$ and then decrease with further increase in cholesterol content. This behavior, which produces a roughly triangular region, reflects a combination of the depression of the melting point of the narrow peak with added cholesterol and the progressive broadening and decrease in the size of the transition as the cholesterol content increases. The presence of a broad transition at cholesterol concentrations above $X_c \simeq 20$ is seen as a prominent region of isotherms which are widely spaced but gradually diminish in separation as X_c increases. Uniform spacing, indicative that no transition is taking place, does not appear to be achieved until about 50% cholesterol.

Although the 15 dilatometer runs plotted in Figure 3 are adequate to describe the major features of the system, it is possible that more details might be revealed by additional runs at more closely spaced concentration intervals. This possibility is particularly likely in the neighborhood of $X_c \simeq 20$, where an abrupt (discontinuous) order-of-magnitude increase in the diffusion coefficient of a fluorescent probe has been reported (Rubenstein et al., 1979). This crucial region was therefore investigated in more detail by direct observation of buoyancies in H_2O–D_2O mixtures. The centrifugation approach used to construct Figure 4 is inappropriate for this purpose because of inadequate temperature control. Instead, patterns of flotation and sedimentation in a water bath controlled to 0.01 °C were recorded. This was carried out in the manner described under Materials and Methods. A typical pattern indicated a sudden decrease in $\bar{V}_a$ of about 0.003 mL g^{-1} at $X_c = 17.5$ and 10 °C. At 20 °C the discontinuity in $\bar{V}_a$ occurs at $X_c = 18.0$ and at 27 °C at $X_c = 18.5$. For all temperatures the discontinuity in $\bar{V}_a$ was approximately the same in magnitude. If this temperature dependence holds at temperatures above 27 °C, the effect would occur at about $X_c = 20$ at 40 °C, the approximate cholesterol concentration at which the narrow DPPC-like component disappears from the transition observed dilatometrically and calorimetrically.

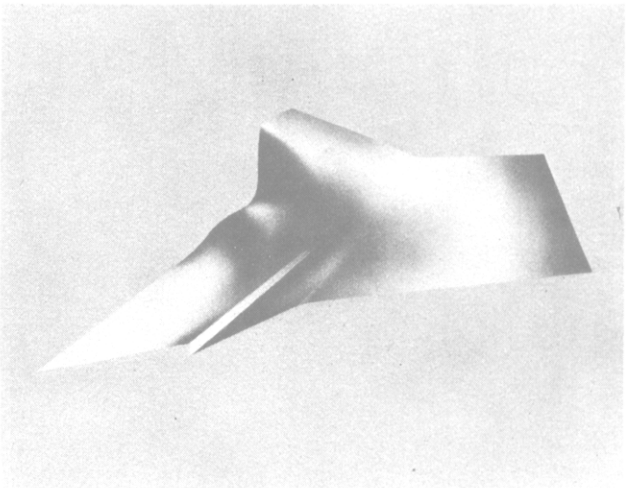

FIGURE 5: X_c–T–$\bar{V}_a$ surface of DPPC–cholesterol bilayers. The surface was designed to emphasize the major features of this study and to present these features in perspective; scaling is approximate. The x axis is mole fraction of cholesterol (X_c) from 0 to 50, the y axis is temperature (T) from 0 to 50 °C, and the z axis is apparent partial specific volume ($\bar{V}_a$). This surface was rendered from a plasticene model constructed according to the raw data presented in Figure 3 and the buoyancy studies described in the text. It is meant to be viewed as if illuminated from the upper right quadrant.

An X_c–T–$\bar{V}_a$ surface constructed from the data obtained in this study is presented in Figure 5. Since the rendering is designed to emphasize the major features discussed earlier and to present these features in perspective, scaling is approximate. The surface is meant to be viewed as if illuminated from the upper right quadrant. Clearly shown are the decrease in size of the abrupt DPPC transition with increasing X_c until it vanishes at about 20% cholesterol and the growth of a broad transition which persists well above $X_c = 20$. Also depicted are the planar regions at the lower temperatures for $0 < X_c < 20$ and $29 < X_c < 50$ and the intermediate region of greater slope at $20 < X_c < 29$. The discontinuity in $\bar{V}_a$ in the neighborhood of 20% cholesterol is seen as a saw-tooth notch extending from the bottom of the surface to the region of the thermotropic transition, although the upper end of the notch is deliberately shaded to indicate extrapolation beyond 27 °C.

Discussion

The effects of cholesterol upon the thermotropic transitions detected by the dilatometer are essentially the same as those found calorimetrically by Mabrey et al. (1978) and similar to those of Estep et al. (1978). The temperature of the abrupt order/disorder transition characteristic of pure DPPC is slightly depressed by about 1 °C at very low cholesterol concentrations in the neighborhood of $X_c = 2$. Within the limits of the technique, the width of this narrow transition is not increased by added cholesterol. However, its size (i.e., $\Delta\bar{V}_a$) appears to decrease linearly with increasing cholesterol content until it vanishes at $X_c \simeq 20$. Concurrent with the steady decrease in size of the narrow DPPC-like transition is the growth of a broader transition which is centered about 1 °C above the narrow one; although the size of this broader transition increases with increasing cholesterol content below $X_c \simeq 20$, the temperature at which it occurs appears to be invariant. These results are most straightforwardly interpreted in terms of a two-phase system below $X_c \simeq 20$, one of pure or nearly pure DPPC and the other of a 4:1 DPPC–cholesterol

complex. This 4:1 complex undergoes a thermotropic transition at about 41 °C. At $X_c = 20$ only a broad transition exists, but it occurs at progressively higher temperatures as the cholesterol level is increased above 20%, while at the same time it increases in width and decreases in size. The data clearly show it to persist at $X_c = 40$, where its midpoint is above 50 °C. There is some evidence that it may persist up to nearly 50 mol % cholesterol, although the data are not sufficiently precise beyond 40% to assure certainty.

Measurements of $\Delta\bar{V}_a$ during the thermotropic transition give essentially the same description of the thermotropic transitions as do changes in ΔC_p. However, dilatometry also gives insight into cholesterol-induced changes both above and below the melting temperature. In this sense, absolute measurements of $\bar{V}_a$ are analogous to absolute heat capacity measurements and may in fact contain more information than the latter since easily discernible volume changes might not be accompanied by easily discernible changes in heat capacity. Information present in $\bar{V}_a$ measurements is displayed in Figure 5. This rendering of the X_c–T–$\bar{V}_a$ surface formed from the raw data presented in Figure 3 and buoyancy studies made in the region $X_c = 15$–25 allows a clear presentation of $\bar{V}_a$ as a function of X_c and T. Thus, in Figure 5 it is seen that at temperatures both below and above the thermotropic transition an event takes place at $X_c \simeq 20$. At the lower temperatures it appears in the X_c–T–$\bar{V}_a$ surface as a small discontinuity in volume followed by an increase in slope of the X_c–$\bar{V}_a$ plane; at high temperatures, where the system is fluid at all cholesterol concentrations, it is seen at least as a pronounced change in slope. The formation of a 4:1 DPPC–cholesterol complex apparently persists even in the fully fluid state.

A second event, seen as a change in slope at $X_c = 29$, clearly occurs as the cholesterol content is increased at temperatures below the thermotropic transition and takes the form of another change in slope in the X_c–$\bar{V}_a$ plane. A similar change may occur at temperatures above the thermotropic transition (Figure 3), but unfortunately the data are not sufficiently precise to allow a definite conclusion to be drawn. Ample evidence exists in the literature for changes in the properties of the DPPC–cholesterol system in the neighborhood of 20% cholesterol (Shimshick & McConnell, 1973; Opella et al., 1976; Estep et al., 1978; Mabrey et al., 1978; Rubenstein et al., 1979), and some investigations have suggested about 30% as a crucial concentration as well (Engelman & Rothman, 1972; Brûlet & McConnell, 1976; Gershfeld, 1978; Rubenstein et al., 1980). Changes at both 20 and 29% are detected by deuteron resonance (Haberkorn et al., 1977), corresponding to increases in motion of the first and second PC fatty acid chains. The dilatometric results support the existence of two crucial concentrations of cholesterol, one at about 20% and the other at about 29%.

The sudden contraction in volume in the neighborhood of $X_c = 20$ strongly suggests that a cholesterol-dependent phase boundary may occur at that concentration. Examination of the buoyancy determinations in H_2O–D_2O mixtures indicates that the discontinuity occurs at about $X_c = 17.5$ at 9 °C, at about $X_c = 18.0$ at 20 °C, and at about $X_c = 18.5$ at 27 °C. At 40 °C it would be expected to occur at about $X_c = 20$, and it seems likely that the disappearance of a pure DPPC component and the occurrence of the phase boundary are associated. The existence of a phase boundary is supported by [^{13}C]cholesterol resonance (Opella et al., 1976), electron spin resonance (Shimshick & McConnell, 1973), and [^{2}H]DPPC resonance studies (Haberkorn et al., 1977) and by measurements of diffusion coefficients (Rubenstein et al., 1979). The weak temperature dependence of the effect seen in the buoyancy studies was also detected by deuteron resonance (Haberkorn et al., 1977).

Since the volume discontinuity is small (0.003 mL g^{-1}, about the size of the pretransition in pure DPPC), it is possible that the event is not representative of the system as a whole, but instead might be a larger effect in only one component of a heterogeneous system. However, the deuteron resonance results indicate an all-or-none phenomenon involving the entire system (Haberkorn et al., 1977); the results of ^{13}C resonance can be similarly interpreted (Opella et al., 1976). The problem of heterogeneity is in fact an important consideration for interpreting any of the observed events. Heterogeneity in density has been reported for DMPC–cholesterol suspensions prepared by dialysis from methanol (Gershfeld, 1978). However, as previously pointed out, all preparations used in the studies reported here produced single, narrow bands by isopycnic density gradient centrifugation, while preparations dialyzed from methanol did not. Additional evidence for density homogeneity, at least in the range $15 < X_c < 25$, comes from the buoyancy studies used to establish the discontinuity in $\bar{V}_a$. Given sufficient time, samples were always observed to either float or sink completely, leaving behind a clear subnatant or supernatant liquid. Since temperature changes of 0.5 °C were sufficient to cause the lipid to change from floating or sinking in a particular tube, density inhomogeneities must have been less than 0.005 mL g^{-1}. The available evidence therefore indicates that all of the reported effects of cholesterol are representative of the system as a whole.

If the discontinuity in $\bar{V}_a$ at $X_c \sim 18$–20 actually represents a cholesterol-induced phase boundary, it may prove useful to think of DPPC–cholesterol mixtures as belonging to either of two quite distinct systems. The first system extends from $0 < X_c \lesssim 20$ and consists of patches of nearly pure DPPC melting abruptly at about 40 °C and patches of a 4:1 DPPC–cholesterol complex melting with a broad transition centered at about 40 °C. The second system extending from $20 \lesssim X_c < 50$ is characterized by a broad symmetrical transition which for $X_c \sim 20$ has a maximum at about 41.5 °C. With increasing X_c this transition broadens, shifts up in temperature, and decreases in size, disappearing most likely at $X_c \simeq 50$. In the $20 < X_c < 50$ region an event occurs at $X_c = 29$. Below the thermotropic transition it appears as a decrease in rate of change of bilayer $\bar{V}_a$ with increasing bilayer cholesterol content.

Evidence exists that an event occurring at $X_c \sim 18$–20 may occur in phospholipids other than just DPPC. Rubenstein et al. (1979) have demonstrated an event at $X_c \sim 18$–20 in bilayers of DPPC and DMPC, as well as egg PC with its mixture of unsaturated and saturated fatty acyl chains.

References

Ahlberg, J., Nilson, E., & Walsh, J. (1967) *The Theory of Splines and Their Applications*, Academic Press, New York.

Bittman, R., & Blau, L. (1972) *Biochemistry 11*, 4831–4838.

Blazyk, J. F., Melchior, D. L., & Steim, J. M. (1975) *Anal. Biochem. 68*, 586–599.

Brûlet, P., & McConnell, H. M. (1976) *J. Am. Chem. Soc. 98*, 1314–1318.

Copland, B. R., & McConnell, H. (1980) *Biochim. Biophys. Acta 599*, 95–109.

Demel, R. A., & de Kruyff, B. (1976) *Biochim. Biophys. Acta 457*, 109–132.

Engelman, D. M., & Rothman, J. E. (1972) *J. Biol. Chem. 247*, 3694–3697.

Estep, T. N., Mountcastle, D. B., Biltonen, R. L., & Thompson, T. E. (1978) *Biochemistry 17*, 1984-1989.
Gebhardt, C., Gruler, H., & Sackman, E. (1977) *Z. Naturforsch., C: Biosci. 32C*, 581-596.
Gershfeld, N. L. (1978) *Biophys. J. 22*, 469-488.
Green, G. (1977) *Int. Rev. Biochem. 14*, 101-152.
Haberkorn, R. A., Griffin, R. G., Meadows, M. D., & Oldfield, E. (1977) *J. Am. Chem. Soc. 99*, 7353-7355.
Hauser, H., & Phillips, M. C. (1979) *Prog. Surf. Membr. Sci. 13*, 297-413.
Hinz, H.-J., & Sturtevant, J. M. (1972) *J. Biol. Chem. 247*, 3697-3700.
Huang, C.-H. (1977) *Lipids 12*, 348-356.
Hui, S. W., & Parsons, D. (1975) *Science (Washington, D.C.) 190*, 383-384.
Ladbrooke, B. D., Williams, R. M., & Chapman, D. (1968) *Biochim. Biophys. Acta 150*, 333-340.
Lee, A. G., Birdsall, N. J. M., Metcalfe, J. C., Toon, P. A., & Warren, G. B. (1974) *Biochemistry 13*, 3699-3705.
Mabrey, S., Mateo, P. L., & Sturtevant, J. M. (1978) *Biochemistry 17*, 2464-2468.
MacDonald, A. G. (1978) *Biochim. Biophys. Acta 507*, 26-37.
Melchior, D. L., & Steim, J. M. (1976) *Annu. Rev. Biophys. Bioeng. 6*, 205-238.
Melchior, D. L., & Czech, M. P. (1979) *J. Biol. Chem. 254*, 8744-8747.
Melchior, D. L., & Steim, J. M. (1979) *Prog. Surf. Membr. Sci. 13*, 211-296.
Melchior, D. L., Scavitto, F. J., Walsh, M. T., & Steim, J. M. (1977) *Thermochim. Acta 18*, 43-71.
Nagle, J. F., & Wilkinson, D. A. (1978) *Biophys. J. 23*, 159-175.
Opella, S. J., Yesinowski, J. P., & Waugh, J. S. (1976) *Proc. Natl. Acad. Sci. U.S.A. 73*, 3812-3815.
Phillips, M. C., & Finer, E. G. (1974) *Biochim. Biophys. Acta 356*, 199-206.
Ranck, J. L., Mateu, L., Sadler, D. M., Tardieu, A., Gulik-Krzywicki, T., & Luzzati, V. (1974) *J. Mol. Biol. 85*, 249-277.
Razin, S., & Rottem, S. (1978) *Trends Biochem. Sci. 3*, 51-55.
Rubenstein, J. L. R., Smith, B. A., & McConnell, H. M. (1979) *Proc. Natl. Acad. Sci. U.S.A. 76*, 15-18.
Rubenstein, J. L. R., Owicki, J. C., & McConnell, H. M. (1980) *Biochemistry 19*, 569-573.
Scheidler, P. J., & Steim, J. M. (1975) *Methods Membr. Biol. 4*, 77-95.
Shah, D. O., & Schulman, J. H. (1967) *J. Lipid Res. 8*, 215-226.
Sheetz, M. P., & Chan, S. I. (1972) *Biochemistry 11*, 4573-4581.
Shimshick, E. J., & McConnell, H. M. (1973) *Biochem. Biophys. Res. Commun. 53*, 446-451.
Steim, J. M. (1974) *Methods Enzymol. 32B*, 262-272.
Vaskovsky, V. E., & Kastetsky, E. Y. (1968) *J. Lipid Res. 9*, 396.
Verkleij, A. J., Ververgaert, P. H. J. Th., de Kruyff, B., & Van Deenen, L. L. M. (1974) *Biochim. Biophys. Acta 373*, 495-501.

Occurrence of a Reduced Nicotinamide Adenine Dinucleotide Oxidase Activity Linked to a Cytochrome System in Renal Brush Border Membranes†

Guillermo Giménez-Gallego, Jesús Benavides, María Luisa García, and Fernando Valdivieso*

ABSTRACT: NADH oxidase activity has been detected in luminal membrane derived from the proximal tubules of rat kidney (brush border membranes). The cytochromes associated with these membranes [García, M. L., Benavides, J., Valdivieso, F., Mayor, F., & Giménez-Gallego, G. (1978) *Biochem. Biophys. Res. Commun. 82*, 738-744] were reduced by NADH, the extent of this reduction being affected by the presence of oxygen and by inhibitors of this NADH oxidase activity. These results suggest that the cytochromes act as an electron transport system between NADH and oxygen. The possibility of mitochondrial contamination is excluded on the basis of differential sensitivity to inhibitors and marker enzyme activities.

The existence of cytochromes in nonmitochondrial membranes of eukaryotic cells is well documented. Berezney et al. (1972) and Berezney & Crane (1972) have reported the presence of cytochromes in the nuclear membrane, and there is considerable information about microsomal cytochromes. NADH dehydrogenase activities have also been described in a wide variety of plasma cell membranes [for an excellent review, see Crane et al. (1979)]. In some cases it has been reported that these plasma membrane NADH dehydrogenases can utilize oxygen as a terminal electron acceptor (Gayda et al., 1977).

In a previous paper (García et al., 1978) we have reported the existence of cytochromes in a specialized plasma membrane, the luminal membrane derived from the proximal tubules of rat kidney (brush border membranes). These cytochromes could only be partially reduced by NADH, and the preparation did not show appreciable rates of NADH-dependent oxygen reduction. Several modifications of the procedure used to prepare a brush border membrane fraction with

† From the Departamento de Fisiología Vegetal, Facultad de Ciencias, Universidad Autónoma de Madrid (G.G.-G.), and the Departamento de Bioquímica y Biología Molecular, Centro de Biología Molecular, Universidad Autónoma de Madrid (J.B., M.L.G., and F.V.), Madrid-34, Spain. *Received January 30, 1980.* This work was supported in part by a grant from Comisión Administradora del Descuento Complementario (I.N.P.).

0006-2960/80/0419-4834$01.00/0